Journal of Catalysis **203,** 264–272 (2001)
doi:10.1006/jcat.2001.3351, available online at http://www.idealibrary.com on IDEAL®

Correlation of Oxidation States in $LaFe_xNi_{1-x}O_{3+\delta}$ Oxides with Catalytic Activity for H_2O_2 Decomposition

H. Falcón,* R. E. Carbonio,*,[1] and J. L. G. Fierro†

*Instituto de Investigaciones en Fisicoquímica de Córdoba (INFIQC), Departamento de Fisicoquímica, Facultad de Ciencias Químicas, Universidad Nacional de Córdoba, Ciudad Universitaria, 5000 Córdoba, Argentina; and †Instituto de Catálisis y Petroleoquímica, CSIC, Cantoblanco, 28049 Madrid, Spain

Received October 16, 2000; revised June 11, 2001; accepted June 11, 2001

Mixed oxides of the type $LaFe_xNi_{1-x}O_3$ with a perovskite structure were prepared by thermal decomposition of citrate mixtures at temperatures ranging from 773 to 1373 K. Temperature-programmed reduction profiles showed a low temperature step (450–500 K) due to the reduction of Ni^{3+} to Ni^{2+} and a high temperature step (650–1170 K) associated with the reduction of Ni^{2+} to Ni^0 and Fe^{3+} to Fe^0. From the microgravimetric reduction profiles it was established that the samples exhibit oxidative nonstoichiometry $LaFe_xNi_{1-x}O_{3+\delta}$ with $\delta = 0.00$–0.08. All the catalysts were tested in the heterogeneous decomposition of hydrogen peroxide ($H_2O_2 \rightarrow H_2O + 1/2\ O_2$) in alkaline medium. It was found that the active sites for the reaction are the highly oxidized transition metals (Ni^{III} and Fe^{IV}). The concentration of these sites, as determined by iodometric titration, varied with catalyst composition and also with the calcination temperature of the precursors. The compensation effect was observed in all the catalysts investigated for hydrogen peroxide decomposition. The appearance of this effect was interpreted in terms of the catalytic reaction occurring on a heterogeneous catalytic surface, that is, a surface with active sites bearing different activation energies.

Key Words: **$LaFe_xNi_{1-x}O_3$ perovskites; compensation effect; H_2O_2 decomposition; oxygen nonstoichiometry; temperature-programmed reduction.**

INTRODUCTION

Perovskite-type oxides (general formula ABO_3) have been used in catalysis as model catalysts (1) as well as real catalysts (2). One of the more successful practical applications is their use as combustion catalysts, applied in exhaust gas cleaning and in diminishing the temperature in burners. The reason for the catalytic versatility of perovskite oxides, together with their stability at high temperature, lies mainly in the high mobility of oxygen and the stabilization of unusual cation oxidation states in this structure. Both properties lead to oxygen nonstoichiometry in the structure. Regulation of these characteristics could be done by appropriate partial substitution of cations in A and B positions. The substitution in B position has the additional advantage that the cation in these sites usually has an important role in the catalytic mechanism. For instance, the intrinsic activity for CH_4 combustion (mole CH_4 coverted per square meter and minute) on $La_{1-x}Sr_xNiO_3$ oxides was strongly dependent on the substitution degree (x) (3). Thus, the intrinsic activity at 773 K was twofold on the $La_{0.9}Sr_{0.1}NiO_3$ with respect to its unsubstituted ($LaNiO_3$) counterpart. The partial substitution of Sr by La led to a modification of the oxide stoichiometry, resulting in a mixture of Ni^{II}/Ni^{III} oxidation states and oxygen vacancies. Marchetti and Forni (4) reported that the catalytic activity of the series $La_{1-x}A_xMnO_3$ (A = Sr, Eu, and Ce) is due to two kinds of oxygens: an adsorbed oxygen species, that reacts at low temperature, and a lattice oxygen species, that becomes available at high temperature booting the catalytic activity.

These perovskite-type oxides also show electrocatalytic activity for oxygen reduction. This reaction is very important in fuel cells and air batteries (5–7). On carbon, oxygen is reduced mainly through the two-electron reaction mechanism, to form hydrogen peroxide (8). Consequently, the catalyst incorporated into the carbon-based electrode must be effective at decreasing the hydrogen peroxide concentration in order to reach sufficiently high operation potentials. So far, we have investigated the hydrogen peroxide decomposition on $LaFe_xNi_{1-x}O_3$ (9). It was found that the active sites are the highly oxidized transition metals (Ni^{3+}, Fe^{4+}) present in the solid. The $LaFe_{0.25}Ni_{0.75}O_3$ showed the optimum catalytic activity and the presence of the highly oxidized Fe^{4+} in the structure was shown using Mossbauer spectroscopy (10). The proposed mechanisms for hydrogen peroxide decomposition (11–15) are based on cyclic electron-transfer processes, in which an electron is transferred from a reduced site on the surface of the catalyst to the peroxide ion yielding an $OH^{\bullet}$ radical, and another electron is transferred from the peroxide ion to an oxidized site on the surface of the catalyst to produce an $HO_2^{\bullet}$ radical.

[1] To whom correspondence should be addressed. Fax: 54 351 4334188. E-mail: carbonio@fisquim.fcq.unc.edu.ar.

0021-9517/01 $35.00

We have previously shown (16) by Rietveld analysis of the X-ray diffraction patterns of the whole $LaFe_xNi_{1-x}O_3$ series that the samples are monophasic for all compositions, except for $x = 0.5$. Those with $x < 0.5$ have the rhombohedral $LaNiO_3$ structure, space group R3c. Samples with $0.5 < x \leq 1$ have the orthorhombic $LaFeO_3$ structure, space group Pnma. Only for $LaFe_{0.50}Ni_{0.50}O_3$ both phases, orthorhombic and rhombohedral, were identified simultaneously. Cell parameters increase with Fe content and normalized cell volume increases linearly with x due to the larger radius of Fe^{3+} (high spin) compared with Ni^{3+} (low spin).

A large variety of Ni perovskite systems $(R,A)NiO_{3-\delta}$, prepared at 1273 K under 200 bar of O_2 pressure, with oxidation states for Ni between 2+ and 4+ were studied to look for correlations between the catalytic activity and the Ni oxidation state or the electrical behavior (17). Those studies confirmed that the active sites for hydrogen peroxide decomposition on Ni-containing perovskite are the highly oxidized transition-metal cations, as shown from the evolution in activity for the $La_{1-x}A_xNiO_3$ series: decomposition rate progresssively increases as the content in highly oxidized Ni (in oxidation states 3+ and 4+) becomes higher.

On the basis of these previous reports, in the present work the rate constants for HO_2^- decomposition were studied and related to the compensation effect which is a particular interrelationship between k_o (reaction frequency factor) and E_a (activation energy): $\ln k_o = A + B \times E_a$ (A and B constants).

EXPERIMENTAL

Catalyst Preparation

The catalysts were prepared by the citrate decomposition method (9, 18), which consists in adding a concentrated solution of nitrates of the required cations to a concentrated citric acid solution. The solution was evaporated in a rotary evaporator at 363 K. The residual water was removed in a vacuum oven. The precursor thus obtained was a mixture of nitrates of the metallic cations and citric acid, which afterward was thermally treated at the synthesis temperature (T_{sint}) between 773 and 1373 K for 12 h in air and then slowly cooled to room temperature.

Four groups of catalysts were studied. Group A, $LaNiO_3$ prepared at different temperatures ($T_{sint} = 873$, 923, 973, 1073, 1173, 1273, 1373 K); Group B, $LaFe_{0.25}Ni_{0.75}O_3$ also prepared at different temperatures ($T_{sint} = 873, 923, 973, 1073, 1173, 1273, 1373$ K) and samples of different compositions ($LaFe_xNi_{1-x}O_3$ with $x = 0$; 0.1; 0.15; 0.25; 0.40; 0.50; 0.75; 0.90; 1.0) prepared at (Group C) $T_{sint} =$ 1073 K and (Group D) $T_{sint} = 1173$ K.

Catalytic Activity for H_2O_2 Decomposition

The measurement of the rate for the hydrogen peroxide decomposition reaction was carried out by measuring the volume of evolved O_2 as a function of time. The experimental setup was similar to that described previously (19, 20). The concentration of HO_2^- ($C_{HO_2^-}$) at time t is calculated as

$$C_{HO_2^-} = C_o - \left[2p_{O_2}V_{O_2}/RTV_{sol}\right], \quad [1]$$

where C_o is the initial concentration of HO_2^-, V_{O2} is the volume of evolved O_2 at time t, V_{sol} is the volume of solution, and P_{O2} is the O_2 partial pressure (atmospheric pressure corrected for the water vapor pressure). A small amount of catalyst (5–20 mg) was dispersed in 45 ml of O_2^--saturated KOH (Merck p.a.) solution at room temperature. A 5-ml aliquot of 0.70 M hydrogen peroxide standard solution presaturated with O_2 was injected into the reaction vessel containing the stirred suspension of the catalysts. The oxygen evolution rate was monitored as a function of time at a given temperature. The measurements were performed between 275 and 353 K.

For the hydrogen peroxide decomposition reaction:

$$HO_{2(aq)}^- \rightarrow 1/2O_{2(g)} + OH_{(aq)}^-. \quad [2]$$

The rate constant which is calculated directly from experimental data is the pseudo-homogeneous first-order rate constant $k_{hom}(s^{-1})$, defined as

$$k_{hom} = d\left(\ln C_{HO_2^-}\right)/dt \quad [3]$$

The heterogeneous rate constant k_{het} is then calculated from k_{hom} as follows

$$k_{het} = [V_{sol} \cdot k_{hom}]/[w_{cat} \cdot (A/w)_{cat}], \quad [4]$$

where w_{cat} is the weight of catalyst used and $(A/w)_{cat}$ the specific area for the catalyst.

Catalysts Characterization

The structural characterization was made by powder X-ray diffraction with a Seifert 3000 P vertical diffractometer using nickel-filtered $CuK\alpha(\lambda = 0.15406$ nm) radiation. The step scans were taken at 2θ angles from 20 to 75° in 2θ. The nitrogen-adsorption isotherms were determined at 77 K in a Micromeritics ASAP 2000. Specific areas were calculated by applying the BET method to these isotherms, taking a value 0.164 nm^2 for the cross section of the N_2-adsorbed molecule. The BET areas of the catalysts used in the present study are summarized in Table 1.

The morphology of the particles was studied by scanning electron microscopy (SEM) using a JEOL Model 35C scanning microscope. The electron gun was operated at energy of 25 keV. A Micromeritics TPD/TPR 2900 apparatus was used for the temperature-programmed reduction

TABLE 1

BET Surface Area of Catalysts

Catalyst	Calcination temperature (K)	S_{BET} (m^2/g)
Group A		
	873	7.3
	923	5.2
$LaNiO_3$	973	4.9
	1173	2.4
	1273	1.9
	1373	1.0
Group B		
	873	10.0
	923	6.5
	973	4.9
$LaFe_{0.25}Ni_{0.75}O_3$	1073	4.8
	1173	3.8
	1273	2.2
	1373	2.0
Group C		
$LaNiO_3$	1073	2.4
$LaFe_{0.10}Ni_{0.90}O_3$	1073	3.6
$LaFe_{0.15}Ni_{0.85}O_3$	1073	2.2
$LaFe_{0.25}Ni_{0.75}O_3$	1073	3.8
$LaFe_{0.40}Ni_{0.60}O_3$	1073	1.7
$LaFe_{0.50}Ni_{0.50}O_3$	1073	1.4
$LaFe_{0.60}Ni_{0.40}O_3$	1073	2.0
$LaFe_{0.75}Ni_{0.25}O_3$	1073	4.9
$LaFe_{0.90}Ni_{0.10}O_3$	1073	3.7
$LaFeO_3$	1073	3.3

(TPR) analysis. Reduction profiles were obtained by passing a 5% H_2/Ar flow at a rate of 50 mL (STP) min^{-1} through the sample (weight around 30 mg). The temperature was increased from 300 to 1050 K at a rate of 10 K min^{-1}, and the amount of hydrogen consumed was determined on a thermal conductivity detector (TCD) as a function of temperature. The TCD signal was calibrated using CuO (Spex) as a standard. Some surface carbonate structures were revealed by photoelectron spectroscopy (binding energy of C 1s at 289.3 eV), but the proportion was too low (e.g., 6.1 CO_3^{2-} entities per 100 La atoms for the $LaNiO_3$ calcined at 1173 K). These carbonate structures appear to be developed only at the surface because no X-ray difftaction lines of La-carbonate could be revealed. The weight loss of the samples in a reducing atmosphere was evaluated in a Stanton STA 781 flow microbalance. The weight change of the samples (ca. 20 mg) was recorded upon heating at a rate of 5 K min^{-1} up to 900 K in a stream of 50 mL (STP) min^{-1} of H_2 gas.

The percentage of $Ni^{III} + Fe^{IV}$ referred to the total transition metals present in each sample (% $Ni^{III} + Fe^{IV}$) was determined by iodometry (Table 2) (21). This method involves dissolving the samples in HCl in the presence of potassium iodide in excess. During this process, the Ni^{3+} cation, which is the strong oxidizing agent in solution, becomes immediately reduced to Ni^{2+} oxidizing I^- to I_2. The amount of I_2 released, which is directly correlated to the amount of Ni^{3+}, is subsequently quantitatively determined by redox titration using tiosulfate as titrant agent.

TABLE 2

Specific Area, Nonstoichiometry ($Ni^{III} + Fe^{IV}$), and Crystalline Phases of $LaFe_xNi_{1-x}O_3$ Catalysts Calcined at 1173 K (Group D)

Catalyst	S_{BET} (m^2/g)	% ($Ni^{III} + Fe^{IV}$)	Crystalline phase
$LaNiO_3$	4.3	20	Per(rho)
$LaFe_{0.10}Ni_{0.90}O_3$	1.7	41	Per(rho)
$LaFe_{0.15}Ni_{0.85}O_3$	1.8	30	Per(rho)
$LaFe_{0.25}Ni_{0.75}O_3$	2.3	58	Per(rho)
$LaFe_{0.40}Ni_{0.60}O_3$	2.4	38	Per(rho)
$LaFe_{0.50}Ni_{0.50}O_3$	1.7	33	Per(rho + ort)
$LaFe_{0.75}Ni_{0.25}O_3$	2.8	22	Per(ort)
$LaFeO_3$	3.2	5	Per(ort)

RESULTS AND DISCUSSION

Temperature-Programmed Reduction

TPR profiles of the $LaFe_xNi_{1-x}NiO_3$ catalyst series are displayed in Fig. 1. TPR profiles exhibit two H_2-consumption peaks (500–540 and 650–1170 K), whose intensity and temperature depend on x. In agreement with the microgravimetric experiments of reduction (see the next section), and also with the isothermal kinetic curves of

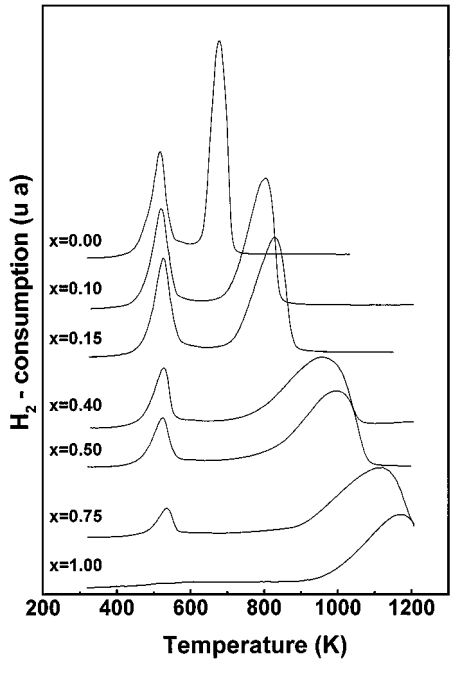

FIG. 1. TPR profiles of $LaFe_xNi_{1-x}O_3$ catalysts calcined in air at 1173 K. (Group D). Experimental conditions were 5% H_2/Ar at a rate of 50 mL (STP) min^{-1}, catalyst weight 30 mg.

reduction reported previously (22), the peak at lower temperatures (500–540 K) is due to reduction of Ni^{3+} into Ni^{2+}, and the peak at higher temperatures is associated with the reduction of Ni^{2+} into metallic Ni^0, but overlaps with the reduction of Fe^{3+}. The broad profile observed for $x \geq 0.4$ and the progressive shift toward higher temperatures with increasing x indicate that the overall reduction of Fe^{3+} ions ($Fe^{3+} \rightarrow Fe^0$) is a complex and activated process which is catalyzed by the formation of metallic Ni^0 particles, probably via a hydrogen spillover process.

X-Ray Diffraction

X-Ray diffractograms of the series indicate that the samples contain the single perovskite phase (Fig. 2). Those with $x < 0.5$ have the rhombohedral distortion (S.G. R3c) evidenced by the splitting of the main peak at 2θ ca. 33° (15) and samples with $0.5 < x < 1$ have the orthorhombic $LaFeO_3$, Pnma structure, evidenced by the small peak at 2θ ca. 24° (15). As previously reported (16) only $x = 0.5$ contains both the rombohedral and orthorhombic phases.

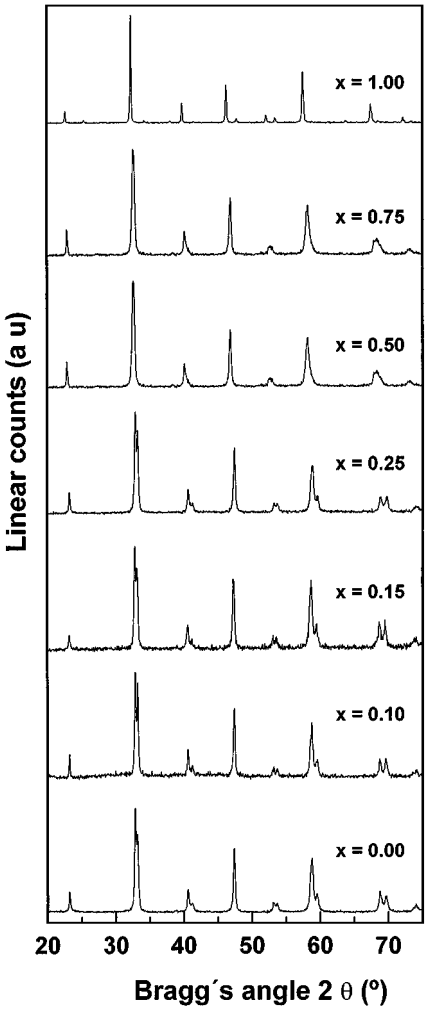

FIG. 2. X-Ray diffraction patterns of $LaFe_xNi_{1-x}O_3$ perovskite oxides calcined in air at 1073 K (Group C). x values indicated in the figure.

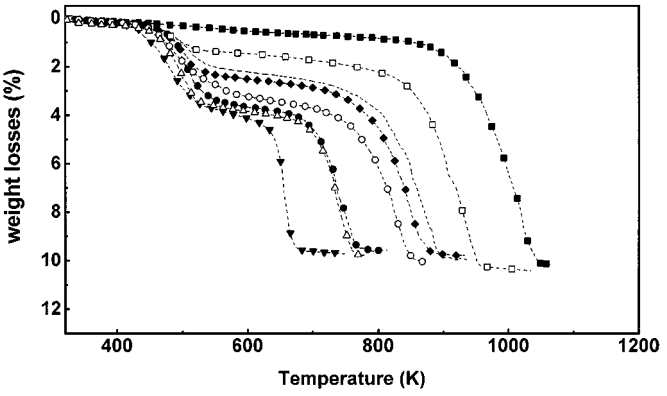

FIG. 3. Weight losses of $LaFe_xNi_{1-x}O_3$ catalysts (Group C) as a function of temperature when heated in a H_2 flow. ▼, $x = 0$; △, $x = 0.10$; ●, $x = 0.15$; ○, $x = 0.25$; ◆, $x = 0.40$; −−, $x = 0.50$; □, $x = 0.75$; ■, $x = 1$.

Oxygen Nonstoichiometry

$LaFe_xNi_{1-x}O_3$ catalysts were treated in a 5% H_2/N_2 flow at temperatures of 900 K while recording the overall weight change. This simple procedure allows not only monitoring of the reduction profiles of the samples but also the quantifying of the extent of the reduction. Figure 3 exhibits the reduction profiles of all the catalysts. From these profiles it is evident that the reducibility of $LaFe_xNi_{1-x}O_{3+\delta}$ oxides depends strongly on x. $LaFeO_{3+\delta}$ exhibited oxidative nonstoichiometry, with the principal reduction step associated to the reduction of Fe^{3+} to Fe^0 taking place at temperatures about 1000 K (23). There was also a small reduction in the 500–700 K range due to the nonstoichiometry of the oxide (oxygen excess and Fe^{4+}). The oxygen excess ($\delta = 0.08$) was lower than that previously reported for the same perovskite prepared at a lower temperature (23, 24), since δ decreased with the calcination temperature. Substitution with Ni led to a decrease in the reduction temperature, which changed from 1000 K for $x = 1$ to 650 K for $x = 0$ ($Ni^{2+} \rightarrow Ni^0$). For the partially substituted ($0.15 \leq x \leq 0.75$) samples, this latter peak overlaps with the reduction of Fe^{3+} into metallic Fe^0. Additionally, a first reduction step appeared in the range 450–500 K, for which the weight change fits well with the theoretical value expected for the quantitative reduction of Ni^{3+} into Ni^{2+}. Working under isothermal conditions, sigmoidal kinetic curves were observed, indicating that the process of reduction can be reasonably described by the shell-type contracting mode. The activation energy for the reduction step in the range 450–500 K was 103 kJ/mol and somewhat higher (111 kJ/mol) for the second peak of reduction placed at higher temperatures.

From these data, the oxygen nonstoichiometry (δ) of the $LaFe_xNi_{1-x}O_{3+\delta}$ oxides was determined. Because the

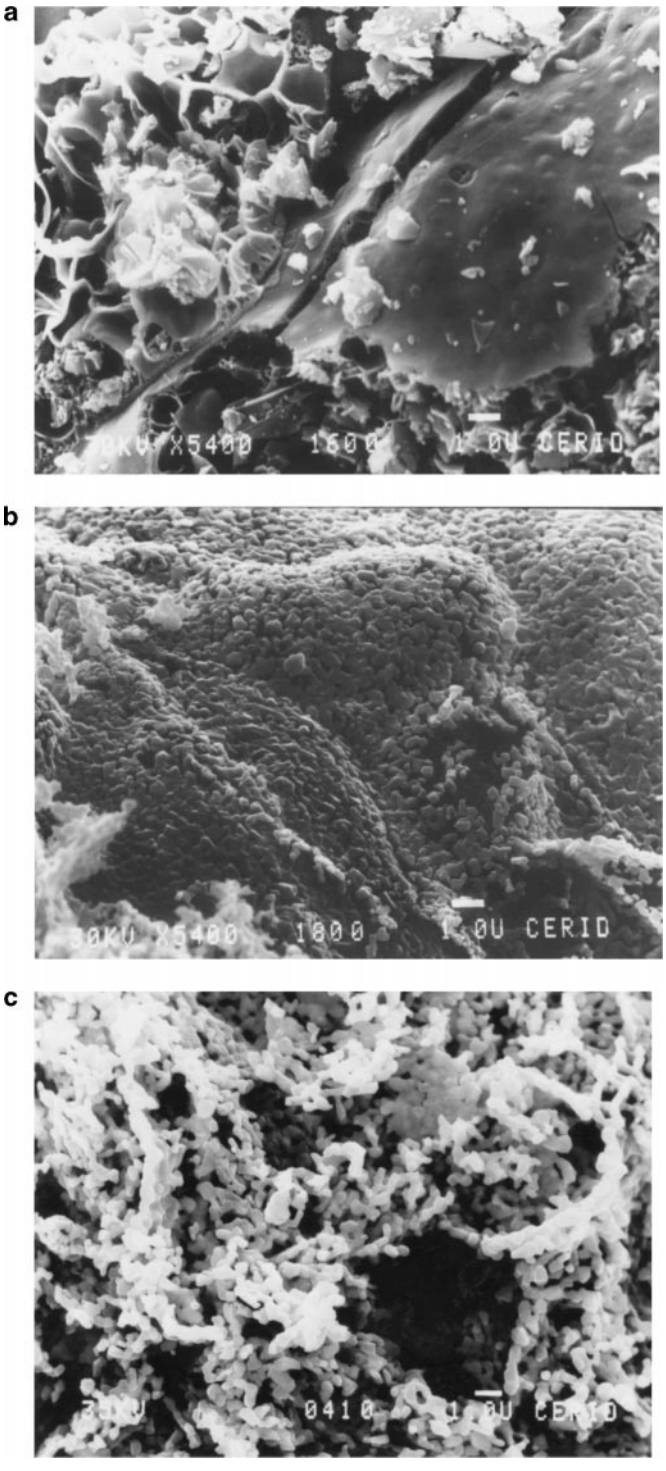

FIG. 4. Microphotographs obtained by SEM for $LaNiO_3$ at T_{sint}.: (a) 873 K (bar = 1 μm); (b) 1073 K (bar = 1 μm); and (c) 1373 K (bar = 1 μm).

weight loss (ΔW) is due to removal of oxygen as water, the oxygen content of the original material can easily be calculated. Thus, the amount of oxygen for a generic $LaFe_xNi_{1-x}O_{3+\delta}$ sample is given by the sum $1.5 + 1.5x + 1.5(1-x) + (\Delta W) = 3 + \delta$, where δ is the oxygen nonstoichiometry number. The δ values indicate an oxidative nonstoichiometry (0.00–0.08), although the tendency does not correlate with x.

SEM Characterization

Figures 4 and 5 show SEM micrographs for $LaNiO_3$ and $LaFe_{0.25}Ni_{0.75}O_3$, respectively, calcined at different temperatures. There is a large change in morphology as the temperature increases. At low calcination temperatures (823–873 K) the catalyst exhibits an "egg shell"-like morphology (see, e.g., Fig. 5a). This characteristic morphology is a consequence of the method of synthesis. There is a step in which a concentrated solution of the metal cation nitrates and citric acid, with a consistency of a viscous syrup, is dried under vaccum (9, 18). During this step microscopic bubbles are formed (see, e.g., Fig. 4a). This morphology is preserved even during grinding of this amorphous precursor. At intermediate calcination temperatures the walls of these bubbles start to crystallize. The poorly defined crystals can be clearly identified in Fig. 4b. At higher calcination temperatures well-defined crystals are formed (Figs. 4c, 5b, and 5c), while at large scale the shape of the bubbles (Figs. 4c and 5b) can be distinguished at these high temperatures.

H_2O_2 Decomposition

In heterogeneous reactions that occur with electron transfer on perovskite-type oxides, the active sites are generally the transition metal ions with partially occupied *d* orbitals (24). The perovskite-type oxides $LaFe_xNi_{1-x}O_3$ can be considered as catalysts with transition metals in mixed oxidation states with the formula $La[Fe^{III}Fe^{IV}]_x[Ni^{III}Ni^{II}]_{1-x}O_{3-\delta}$ where y stands for oxygen vacancies (9). So, from what was stated above, some of these transition ions are expected to be the active sites for hydrogen peroxide decomposition.

Plots of log $c_{HO_2^-}$ vs time are shown in Fig. 6 for two different catalysts. The good linearity indicates first order in HO_2^- concentration. This is in agreement whith results reported in the literature for spinel-type oxides (13, 14) and perovskite oxides (9, 20).

In order to study the probable correlation between the reaction rate and the distribution of active sites, the dependence of the specific rate constant (k_{het}) with the sum percentage $[Fe^{IV} + Ni^{III}]$ was studied for catalysts of different compositions (Group C). The results shown in Fig. 7 exhibit an almost linear increase of the rate constant with the $[Fe^{IV} + Ni^{III}]$. This relationship would indicate that the active sites for hydrogen peroxide decomposition are these highly oxidized transition metal sites. If it is assumed that the highly oxidized sites behave as acceptor centers for electrons, and that their concentration is the main factor that determines the reaction rate, then the rate determining step

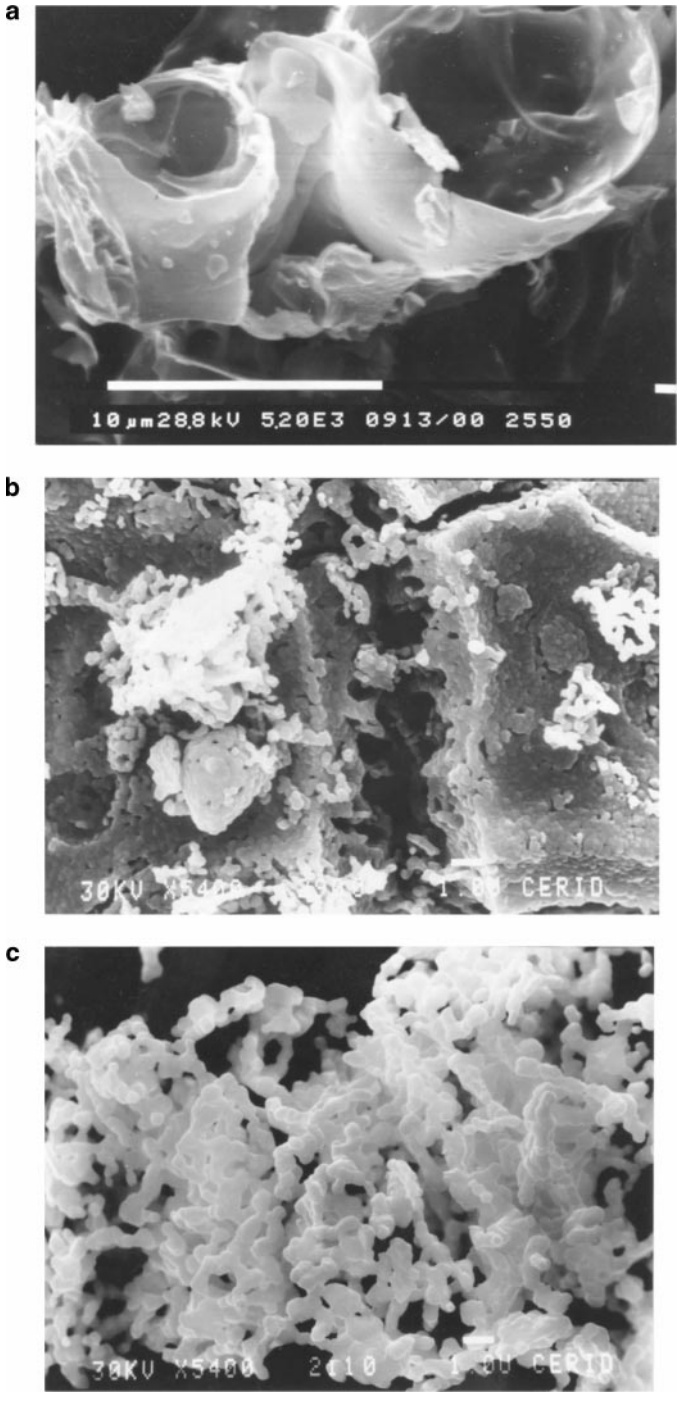

FIG. 5. Microphotographs obtained by SEM for $LaFe_{0.25}Ni_{0.75}O_3$ at T_{sint}.: (a) 823 K (bar = 10 μm); (b) 1173 K (bar = 1 μm); and (c) 1373 K (bar = 1 μm).

for the hydrogen peroxide decomposition would involve these acceptor centers.

Compensation Effect in Heterogeneous H_2O_2 Decomposition

The compensation effect has frequently been observed in heterogeneous catalysis (25, 26). This effect shows a linear

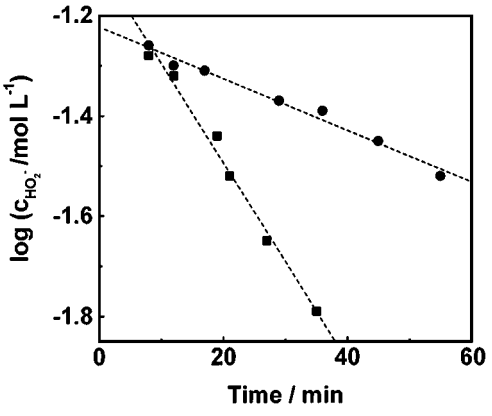

FIG. 6. Log $c_{HO_2^-}$ vs time, m_{cat} = 0.005 g, c_0 = 0.074 M: ●, $LaFe_{0.5}Ni_{0.5}O_3$; and ■, $LaFe_{0.25}Ni_{0.75}O_3$ (Group D).

relationship between log A (where A is the preexponential factor and the activation energy (E_a),

$$\log A = mE_a + c, \qquad [5]$$

when a reaction is studied with different catalysts or when a number of reactions are studied on a catalyst (27, 28). If the compensation relationship is present, then, there must be a characteristic temperature, named isokinetic temperature (T_i), which is expressed as

$$T_i = \frac{1}{2.303Rm}. \qquad [6]$$

At this temperature the reaction proceeds at a rate (k_{iso}) which is the same on all the catalysts (if a reaction on different catalysts is being studied) or for all the reactions (if different reactions are being studied on a catalyst). The value of k_{iso} is obtained from Eq. [5] ($c = \log k_{iso}$). The fastest reaction has the highest activation energy above the isokinetic temperature and the lowest activation energy below the isokinetic temperature (29). If the isokinetic

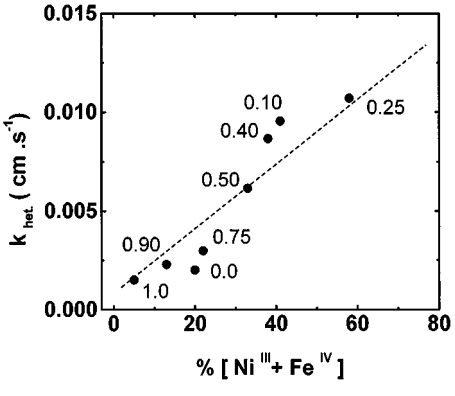

FIG. 7. k_{het} for H_2O_2 decomposition vs % [Ni^{III} + Fe^{IV}] for $LaFe_xNi_{1-x}O_3$ (Group C). x values indicated in the figure.

temperature occurs in the middle of the measured temperature range, the compensation effect can be just a wrong correlation caused by data scattering (30). In order to discard this wrong compensation, linear relationships given by Eq. [5] must be found along with only one intersection in the Arrhenius plots. The lack of a single intersection is indicative of the probable absence of this effect (30, 31). A generally accepted explanation of frequently observed compensation effects in heterogeneous catalysis, first reported by Constable (32), is still missing. Compensation behavior is found not only in heterogeneous catalysis but also in homogeneous reactions (33). This general occurrence should favor the assumption that the compensation effect is best understood as only one single effect with a general mechanistic background, which applies to the whole of chemistry and not only to heterogeneous catalysis (34–39). Among the specific explanations for this effect, the more frequently discussed are: (i) an energetically active surface (40), (ii) linear relations between adsorption enthalpy and adsorption entropy, and (iii) variable surface concentrations of active sites (41). Therefore, it is evident that this is a group of catalysts for which it is possible to obtain a varying amount of active sites by varying the synthesis conditions. On this basis, the compensation effect will be analyzed over the different groups of catalysts.

The log A vs E_a plots obtained for the groups A and B are shown in Figs. 8a and 8b. Linearity of the plots shows that the compensation effect is present in these groups of catalysts. In Fig. 8a (Group A) two well-defined linear regions are observed. This behavior can be explained if it is assumed that two subgroups of catalysts are formed. One would form between 873 and 1073 K and the other between 1173 and 1373 K. This explanation is consistent with the well-known decomposition of $LaNiO_3$ in La_2NiO_4 and NiO, above 1133 K (16, 42), which would yield a mixture of La_2NiO_4 and NiO phases, or a mixture of the three phases La_2NiO_4, NiO, and $LaNiO_3$ if the decomposition reaction is incomplete. In the case of $LaFe_{0.25}Ni_{0.75}O_3$ (Fig. 8b), only one linear region is obtained, indicating that the stability limit would expand up to 1373 K. This fact was also observed by X-ray diffraction (16). This last result could be explained in terms of the fact that the introduction of a small amount of Fe^{III} replacing Ni^{III} in the structure of $LaNiO_3$ allows the compound to be synthesized at higher temperatures without decomposition. This is reasonable bearing in mind that Ni^{III}, which has a high tendency to reduce to Ni^{II} (42), is replaced by Fe^{III} which is highly stable in the perovskite structure. It is reasonable to assume that the change in the temperature of synthesis in these two groups of catalysts may modify the number of sites (to which the preexponential factor is proportional) as well as their activation energies, thus leading to the appearance of a compensation effect.

From the above analysis, and if there is a compensation relationship, there must be an intersecting point common to all the straight lines in a log k vs $1/T$ plot. Otherwise, as noted before, the linear relationship between log A and E_a should be a wrong correlation due to data scattering. Such intersections are shown in Figs. 9a and 9b for two groups of catalysts. From the slope and the ordinate of the log A vs E_a plots the isokinetic parameters T_{iso} and log k_{iso} can be obtained. They are shown in Table 3 along with the correlation coefficients of the linear relationships.

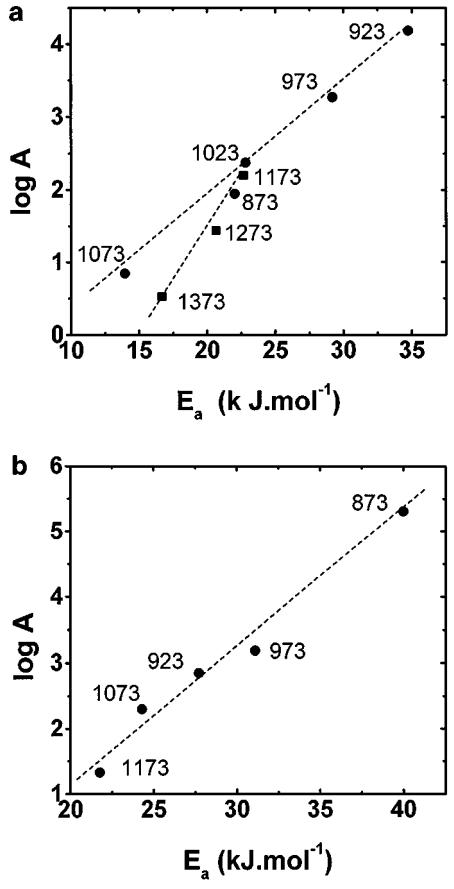

FIG. 8. Compensation relation for H_2O_2 decomposition for the different groups of catalysts. Temperature of synthesis is indicated in the figure. (a) Group A: ●, subgroup 873–1073 K; ■, subgroup 1173–1373 K; (b) Group B.

TABLE 3

Isokinetic Parameters (T_i and log k_{iso}) for the Different Catalyst Groups Derived from the Straight Lines in Figs. 8a and 8b

Catalyst group	T_i (K)	log k_{iso}	r_{corr}
A between 873 and 1073 K	321.5	−1.4440	0.996
A between 1173 and 1373 K	190.0	−4.0783	0.991
B between 873 and 1173 K	253.2	−2.958	0.991

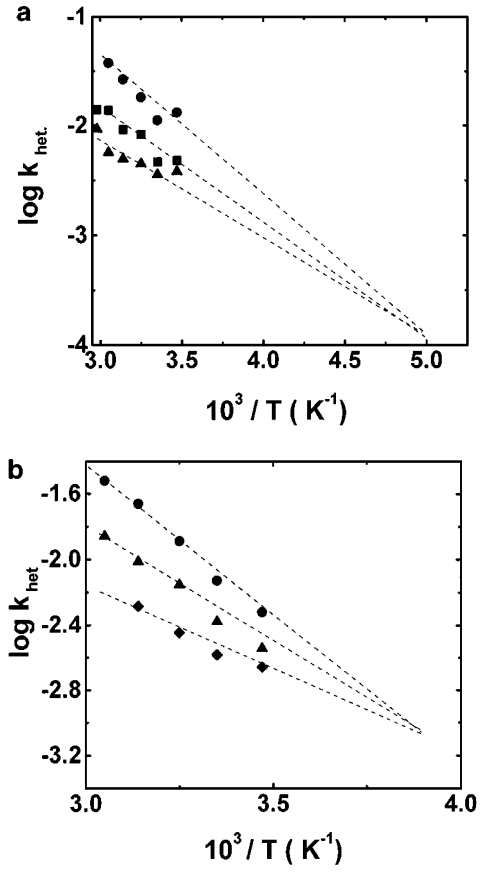

FIG. 9. Arrhenius plots for H_2O_2 decomposition for the different groups of catalysts. (a) Group A: $T_{sint.}$ between 1173 and 1373 K; ●, $T_{sint.}$ = 1173 K; ■, $T_{sint.}$ = 1273 K; ▲, $T_{sint.}$ = 1373 K. (b) Group B: $LaFe_{0.25}Ni_{0.75}O_3$ at ●, $T_{sint.}$ = 873 K; ▲, $T_{sint.}$ = 973 K; ◆, $T_{sint.}$ = 1173 K.

In this particular case we assciate the compensation effect to a variable concentration of active sites, namely FeIII and FeIV, with different activation energies. This concentration can be changed through composition and calcination temperature.

CONCLUSIONS

(i) Catalytic activity for H_2O_2 decomposition on $LaFe_xNi_{1-x}O_3$ perovskites was found to be dependent on the number of highly oxidized transition metal sites. The linear dependence of the rate constant with % [Ni^{III} + Fe^{IV}] suggests that the active sites for H_2O_2 decomposition are these highly oxidized transition metal sites.

(ii) A compensation effect was found for H_2O_2 decomposition on these catalysts. The absence of a false compensation effect was verified through a common intercept in all the log k vs $1/T$ plots. The appearance of this effect was interpreted as due to the existence of a heterogeneous reaction surface with a distribution of active sites with different activation energies (Ni^{III} and Fe^{IV}). The amount of these active sites can be varied by changing catalyst composition and its calcination temperature. For $LaNiO_3$ catalyst prepared at different temperatures, two linear regions were found in the compensation relation. These two regions were assigned to two different sets of catalysts, one between 1173 and 1373 K and the other between 873 K and 1073 K. This explanation is consistent with the decomposition of $LaNiO_3$ in La_2NiO_4 and NiO above 1133 K. On the other hand, $LaFe_{0.25}Ni_{0.75}O_3$ showed only one linear region. This is in agreement with the fact that this compound is stable up to 1273 K, showing only a slight decomposition at 1373 K. The introduction of 25% of iron into the Ni^{III} sites thus increases the thermal stability of this perovskite oxide.

REFERENCES

1. Simont, L., Garin, F., and Maire, G., *Appl. Catal. B.* **11**, 167 (1997).
2. L. G. Tejuca, and Fierro, J. L. G. (Eds.),"Properties and Applications of Perovskite-Type Oxides", Dekker, New York, 1993.
3. De la Cruz, R. M. G., Falcón, H., Peña, M. A., and Fierro, J. L. G., in preparation.
4. Marchetti, L., and Forni, L., *Appl. Catal. B.* **15**, 179 (1998).
5. Prakash, J., Tryk, D., and Yeager, E., *J. Power Sources* **29**, 413 (1990).
6. Lamminem, J., Kivisaari, J., Lamminem, M. J., Viitanem, M., and Vuorisalo, J., *J. Electrochem*. Soc. **137**, 3430 (1990).
7. Carbonio, R. E., Fierro, C., Tryk, D., Scherson, D., and Yeager, E., *J. Power Sources* **22**, 387 (1988).
8. Yeager, E., *J. Mol. Catal*. **38**, 5 (1986).
9. Falcón, H., and Carbonio, R. E., *J. Electroanal. Chem*. **339**, 69 (1992).
10. Falcón, H., Goeta, A. E., Goya, G. F., Mercader, R. E., Punte, G., and Carbonio, R. E., *Hyperfine Interact.* **90**, 371 (1994).
11. Kanungo, S. B., Parida, K. M., and Sant, B. R., *Electrochim. Acta* **26**, 1157 (1981).
12. Gerischer, R., and Gerischer, H., Z. *Phys. Chem. N. F.* **6**, 1978 (1966).
13. Onuchukwu, A. I., *J. Chem. Soc. Faraday Trans. I* **80**, 1447 (1984).
14. Goldstein, J. R., and Tseung, A. C. C., *J. Mater. Sci.* **7**, 1383 (1972).
15. Cota, H. M., Katan, J., Chim, J., and Schoenweis, F. J., *Nature* **203**, 1281 (1964).
16. Falcón, H., Goeta, A. E., Punte, G., and Carbonio, R. E., *J. Solid State Chem*. **133**, 379 (1997).
17. Alonso, J. A., Martínez-Lope, J., Falcón, H., and Carbonio, R. E., *Phys. Chem. Chem. Phys*. **1**, 3025 (1999).
18. Tascón, J. M. D., Mendioroz, S., and Tejuca, L. G., *Z. Phys. Chem. (Wiesbaden)* **124**, 109 (1981).
19. Jiang, S. P., Lin, Z. G., and Tseung, A. C. C., *J. Electrochem. Soc.* **137**, 759 (1990).
20. Carbonio, R. E., Tryk, D., and Yeager, E., "Proceedings, Symp. on Electrode Materials and Processes for Energy Conversion and Storage," Vol. 87-1, p. 238, The Electrochemical Society, Pennington, NJ, 1987.
21. Takahashi, J., Toyoda, T., Ito, T., and Takasu, M., *J. Mater. Sci.* **25**, 1557 (1990).
22. Falcon, H., Baranda, J., Campos-Martin, J. M., Peña, M.A., and Fierro, J. L. G., *Stud. Surf. Sci. Catal.* **130**C, 2195 (2000).
23. Mizusaki, J., Mori, N., Takai, H., Yonemura, Y., Minamiue, H., Tagawa, H., Dokiya, M., Inaba, H., Naraya, K., Sasamoto, T., and Hashimoto, T., *Solid State Ionics* **129**, 163 (2000).
24. Tascón, J. M. D., Fierro, J. L. G., and Tejuca, L. G., *J. Chem. Soc. Faraday Trans. I* **81**, 2399 (1985).
25. Fierro, J. L. G., Tascón, J. M. D., and Tejuca, L. G., *J. Catal.* **93**, 83 (1985).

26. Gaiwey, A. K., *Adv. Catal.* **26**, 247 (1977).
27. Corma, A., Llopis, F., Monton, J. B., and Weller, S. W., *J. Catal.* **141**, 97 (1993).
28. Kemball, C., *Proc. Roy. Soc. A* **217**, 376 (1953).
29. Campelo, J. M., García, A., Luna, D., and Marinas, J. M., *J. Catal.* **97**, 108 (1986).
30. Suárez, M. P., Palermo, A., and Aldao, C. M. J., *Thermal Anal.* **41**, 807 (1994).
31. Linert, W., and Sapunov, V., *Chem. Phys.* **119**, 265 (1988).
32. Constable, F. H., *Proc. Royal Soc. London*, Ser. A **108**, 355 (1925).
33. An explanation of the compensation effect in catalysis can be seen in *J. Catal.* **146**, 310 (1993).
34. Montanari, G. C., and Motori, A., *J. Phys. D* **28**, 1433 (1993).
35. Brudugeac, B., and Segal, E. G. J., *Thermal Anal.* **49**, 1199 (1994).
36. Brudugeac, B., and Segal, E. J., *Thermochim Acta* **202**, 121 (1992).
37. Larson, R., *Catal. Lett.* **16**, 273 (1992).
38. Karpinski, Z., Gandhi, S. N., and Sachtler, W. M. H., *J. Catal.* **141**, 337 (1993).
39. Bond, G. C., Hooper, A. D., Slaa, J. C., and Taylor, A. O., *J. Catal.* **163**, 319 (1996).
40. Cremer, E., *Adv. Catal.* **7**, 75 (1955).
41. Bond, G. C., "Catalysis by Metals," Academic Press, New York, 1962.
42. Odier, P., Nigara, Y., Coutures, G., and Sayer, M., *J. Solid State Chem.* **56**, 32 (1985).
43. González Calvet, J. M., Sayagués, M. J., and Vallet Regi, M., *Solid State Ionics* **32/33**, 72 (1989).